Mechanism of Cyanamide Hydration Catalyzed by Carbonic Anhydrase II Suggested by Cryogenic X-ray Diffraction†

Annalisa Guerri,‡ Fabrizio Briganti,§ Andrea Scozzafava,§ Claudiu T. Supuran,§ and Stefano Mangani*,‡

Dipartimento di Chimica, Università di Siena, Via Aldo Moro, I-53100 Siena, Italy, and Laboratorio di Chimica Inorganica e Bioinorganica, Università di Firenze, Via Gino Capponi 7, I-50121 Florence, Italy

Received April 25, 2000; Revised Manuscript Received July 17, 2000

ABSTRACT: The three-dimensional structure of a possible intermediate in the hydration reaction of cyanamide to urea catalyzed by human carbonic anhydrase II (hCAII) has been determined by cryocrystallographic techniques. The crystal structure shows that two different adducts are formed under the experimental conditions and that they have different occupancy in the crystal. The high occupancy form consists of a binary hCAII−cyanamide complex where the substrate has replaced the zinc-bound hydroxide anion present in the native enzyme, maintaining the tetrahedral geometry around the metal ion. The second, low-occupancy form consists of a hCAII−cyanamide−water ternary complex where the catalytic zinc ion, still being bound to cyanamide, is approached by a water molecule in a five-coordinate adduct. While the first form can be considered a nonproductive complex, the second form may represent an intermediate state of the catalyzed reaction where the water molecule is about to perform a nucleophilic attack on the zinc-activated cyanamide substrate. The structural evidence is consistent with the kinetic data previously reported about this recently described hydrolytic reaction catalyzed by hCAII, and indicates that a different mechanism with respect to that generally accepted for the physiologic carbon dioxide hydration reaction may be adopted by the enzyme, depending on the substrate chemical properties.

The 14 different carbonic anhydrase isozymes (CA,[1] EC 4.2.1.1) or CA-related proteins (CA-RP) described up to now in higher vertebrates, including humans (*1*), are involved in critical physiological processes connected with respiration and transport of CO_2 and bicarbonate between metabolizing tissues and the lungs, pH homeostasis, and electrolyte secretion in a variety of tissues and organs, as well as biosynthetic reactions, such as the gluconeogenesis and ureagenesis among others (*2*, *3*). The availability in the catalytic site of these enzymes of a strong nucleophile, the Zn(II)-bound hydroxide ion, accounts for the experimental evidence which shows that different CA isozymes are able to catalyze a variety of hydrolytic reactions (*4*−*6*). When the high number of known CA isozymes and their important (and many times unknown) physiological functions are taken into account, it is critical to study the different reactions possibly catalyzed by CAs and to design novel types of inhibitors as well as substrates for these versatile enzymes (*6*−*8*). In a previous work, this group reported a new hydrolytic reaction catalyzed by several CA isozymes, i.e., the hydration of cyanamide to urea (*6*). Cyanamide[2] was shown to act as the first potent suicide substrate of these enzymes, since the urea, or the ureate anion, formed after the hydrolytic reaction remains blocked within the enzyme active site where it is directly coordinated to the Zn(II) ion through a protonated nitrogen atom and also forms eight hydrogen bonds with residues Thr199 and Thr200 and three water molecules. These strong interactions at the active site explain why the ureate or urea bound to the Zn(II) cannot be displaced even by high concentrations of the very potent sulfonamide inhibitors (*6*). In the above-mentioned study, we also proposed a reaction mechanism to explain the cyanamide hydration, based on electronic spectroscopy, kinetic, and X-ray crystallographic studies of this system. Still, we were unable to determine the precise cyanamide mode of binding to the enzyme, due to the conversion of this substrate to urea in the crystal during data collection, so that only the latter molecule could be identified in the electron density maps.

The recent advances in protein X-ray cryocrystallographic techniques have opened up the possibility of determining the structures of intermediates in enzyme-catalyzed reactions by freeze-trapping sufficiently stable reaction intermediates that can accumulate in enzymes that are active in the crystalline state. At 100 K, all the enzyme motions that are

† We acknowledge the financial support of the Italian Ministero dell'Università e della Ricerca Scientifica e Tecnologica (MURST, Programmi di ricerca di rilevante interesse nazionale). The financial support of the CNR Target Project on Biotechnology and of CNR Grant 96.01270.PF37 (Gruppo per la Difesa dai Rischi Chimico Industriali) is also gratefully acknowledged.

* To whom correspondence should be addressed: Department of Chemistry, University of Siena, I-53100 Siena, Italy. E-mail: Mangani@unisi.it. Phone: +390577-234255. Fax: +390577-234233.

‡ Università di Siena.

§ Università di Firenze.

[1] Abbreviations: AMS, 3-meruri-4-aminobenzenesulfonamide; CA, carbonic anhydrase; CA-RP, CA-related proteins; hCAII, human carbonic anhydrase II; TRIS, tris(hydroxymethyl)aminomethane; F_o, observed structure factor amplitude; F_c, calculated structure factor amplitude; α, structure factor phase.

[2] Tautomeric forms for the cyanamide molecule: HN═C═NH ↔ H_2N−C≡N.

10.1021/bi000937c CCC: $19.00
Published on Web 10/03/2000

essential for the catalytic reaction are completely frozen so that intermediate species can be indefinitely trapped and investigated (*9*). The kinetic data on the cyanamide hydration catalyzed by human carbonic anhydrase II (hCAII) show that after incubation with a cyanamide solution for 4 h 10% of the substrate is converted to urea and that the reaction is complete after 24 h (*6*). This makes this reaction a suitable candidate for a mechanistic investigation by X-ray crystallography. In this paper, we report the X-ray structure of the adduct of cyanamide with hCAII, obtained by freezing the hCAII crystals soaked in an inhibitor solution, that shows a possible intermediate in the hCAII-catalyzed cyanamide hydration.

MATERIALS AND METHODS

Human CA II (hCAII) cDNA was obtained by overexpression in *Escherichia coli* strain BL21 (DE3) from the plasmid pACA/hCAII as previously described (*10*, *11*). The cell growth protocol was the one described by Lindskog's group (*11*), and the enzymes were purified by affinity chromatography according to the published method (*12*). Enzyme concentrations were determined spectrophotometrically at 280 nm, utilizing a molar absorptivity of 54.00 mM^{-1} cm^{-1} for hCAII (M_r = 29.30 kDa) (*13*).

Crystals of hCAII have been obtained by the hanging drop technique, using a 10 mg/mL solution of protein in 50 mM TRIS-HCl buffer (pH 7.7). The drops consisted of 4 μL of the enzyme solution and 4 μL of the precipitant solution containing 2.3−2.4 M $(NH_4)_2SO_4$ in 50 mM TRIS-HCl (pH 7.7) and 2 mM 4-(hydroxymercury)benzoate to promote the growth of highly ordered crystals. The drops were equilibrated by vapor diffusion against the precipitant solution at 4 °C, and the crystals appeared after 3−4 weeks.

To obtain the hCAII−cyanamide complex, a 50 mM TRIS-HCl-buffered soaking solution (pH 7.7) containing 3 M $(NH_4)_2SO_4$ and 3 M cyanamide was used. The solution kinetic data on the cyanamide hydration catalized by hCAII recently reported indicate that after 4 h about 10% of the cyanamide has been converted to urea at 298 K (*6*). The slowness of the reaction offers the possibility of freezing possible intermediates in the solid state even if the kinetics in the crystal are not known and probably differ from those observed in solution. The nature of the reaction did not allow us to devise a convenient way to accumulate the substrate in the crystal before starting the reaction to obtain maximum occupancy. The reaction is pH-independent within the range where the crystals are stable (pH 6−9) so that a pH jump cannot be used to trigger the reaction when the sites have already reached maximum cyanamide occupancy. The cyanamide hydration reaction was followed by soaking the hCAII crystals in the cyanamide solution described above, for different time intervals ranging between 30 and 360 min. Each crystal was then washed for 30−60 s in a cryoprotecting solution consisting of the precipitant solution with added 15% ethylene glycol and flash-frozen under a cold nitrogen stream (100 K) for X-ray data collection. The soaked crystals are isomorphous with the native enzyme being monoclinic in space group $P2_1$ with cell parameters within 1% of those of the native enzyme (2CBA) having typical cell parameters: a = 42.01 Å, b = 41.43 Å, c = 71.99 Å, and β = 104.4° (*14*).

Table 1: Data Collection Parameters and Refinement Statistics for the hCAII−Cyanamide Complex

data collection method	0.3° ω scans
no. of crystals	1
resolution range (Å)	18.00−1.90
R_{merge}	0.057
no. of raw measurements	37672
no. of unique reflections	17716
redundancy	2.1
completeness (%)	95.0
high-resolution bin (Å)	2.05−1.90
completeness (%)	88.5

Refinement Statistics	target error	HCAII−cyanamide complex
R_{cryst} (R_{free})		0.165 (0.218)
bond distance (Å)	0.020	0.014
angle distance (Å)	0.040	0.034
planar 1−4 distance (Å)	0.050	0.069
miscellaneous		
planar peptide groups	0.030	0.025
planar aromatic groups	0.020	0.012
chiral centers (Å^3)	0.150	0.133
nonbonded distances		
single torsion (Å)	0.30	0.18
multiple torsion (Å)	0.30	0.23
H−Y−H bonds	0.30	0.15
torsion angles		
planar (deg)	7.0	9.9
staggered (deg)	15.0	17.2
orthonormal (deg)	20.0	28.5
thermal restraints		
main chain bond (Å^2)	2.00	1.64
main chain angle (Å^2)	3.00	2.24
side chain bond (Å^2)	2.00	2.04
side chain angle (Å^2)	3.00	3.00

For each crystal, a complete data set was collected to the highest possible resolution (ranging between 1.9 and 1.5 Å), and Fourier maps were calculated with $2F_o - F_c$ and $F_o - F_c$ coefficients where F_c and phases α_{nat} were obtained from the native hCAII model from which the active site residues, the zinc ion, and all the water molecules had been omitted. For each data set, the difference Fourier maps were inspected to seek for the evidence of cyanamide binding before the hydration step. The experiment was considered successful if significant electron density ($>4\sigma$) compatible with a cyanamide molecule bound into the active site was found in the maps. The crystals soaked for 90 min at 279 K provided the desired results. The experiment was repeated three times to check for reproducibility that was always excellent. The data set extending to 1.9 Å resolution was chosen for refinement on the basis of better apparent occupancy of the cyanamide binding sites and for its higher data completeness.

The data have been collected on a Siemens SMART 1K CCD detector using Cu Kα X-ray radiation from a Siemens M12X-HF rotating anode X-ray generator operating at 45 kV and 90 mA. All data collections were performed at 100 K, the temperature being kept constant by an Oxford Cryosystem apparatus. The data collection parameters and the refinement statistics for the chosen data set are reported in Table 1. The CCP4 package (*15*) was used for all calculations. The programs TOM (FRODO adaptation for SGI workstation by S. Oatley) (*16*) and O (*17*) were used for model rebuilding and inspection of the $2F_o - F_c$ and $F_o - F_c$ Fourier maps. The programs REFMAC (*18*) and ARP (*19*) from the CCP4 suite were used for the stereochemically

restrained refinement. The protocol of refinement and model building was that already reported for the hCAII−urea complex (*6*) and comprises several cycles. During refinement, the zinc ion and all its protein and nonprotein ligands were not subjected to any restraint. The last restrained refinement cycle yielded a final *R* factor of 0.165 (R_{free} = 0.218). The final temperature factors of the cyanamide atoms range between 8.6 and 14.1 Å^2. The final model contains 2044 protein atoms, two Hg atoms, one cyanamide molecule, and 246 water molecules. The structure quality was checked by the program PROCHECK (*20*), and the final coordinates have been deposited with the Protein Data Bank under accession number 1F2W. The final $F_o - F_c,\alpha_{calc}$ calculated with the complete hCAII−cyanamide model presented peaks at the 2σ level only in the proximity of the Zn and Hg peaks, indicating anisotropy of their thermal motion. Residual electron density was also present at the N-terminus, where one to three residues were expected, and at the C-terminal regions, but it was not well-defined and prevented any modeling.

RESULTS

The crystal structure of the hCAII−cyanamide complex shows that the overall structure of the hCAII molecule remains unaltered upon interaction with cyanamide, the rms deviation between all the atoms of the native hCAII and those of the complex being 0.28 Å. The zinc itself and its histidine ligands as well as all the relevant residues lining the active site cavity maintain the same conformation as in the native enzyme. The only relevant changes occur in the structure of the solvent present in the active site and in the zinc coordination polyhedron. In native hCAII, a Zn^{2+} ion is bound to three histidine residues (His94, His96, and His119) and to a water or hydroxide molecule in an almost regular tetrahedral coordination geometry (*14*). An initial Fourier difference map revealed the presence of an elongated electron density at a 5σ level at the zinc site. The density could be exactly fitted by a model of the linear cyanamide molecule bound to the zinc ion by replacing the zinc-bound water or hydroxide molecule of the native enzyme (Wat263 in the 2CBA nomenclature). Additional, weaker electron density (~2.5σ) compatible with a water molecule appeared within contact distance from zinc and cyanamide. As the initial enzyme model (consisting of hCAII residues 4−261, the zinc ion, and a Hg atom from the mercury *p*-hydroxybenzoate molecule bound to the Cys206 sulfur) was refined, the electron density in the active site became clearer. This electron density had a spherical shape and could be attributed to a water molecule (or related species) located in a place never previously observed, in native hCAII or in any of its adducts crystallographically determined so far. A water molecule (Wat51) was added in this position to the model and refined at full occupancy. The Wat51 final temperature factor is 46.2 Å^2, which compared to those of the other atoms bound to zinc (cyanamide N2, 8.6 Å^2; His94 Nϵ2, 7.9 Å^2; His96 Nϵ2, 3.3 Å^2; His119 Nδ1, 4.1 Å^2; Zn, 6.0 Å^2) indicates partial occupancy. This suggests that, while cyanamide almost fully occupies the hCAII sites in the crystal, the ternary Zn(II)−cyanamide−Wat51 complex is present in only a fraction of the sites. In other words, it appears that two distinct hCAII−cyanamide adducts are observed in the crystal: a binary hCAII−cyanamide complex and a ternary hCAII−cyanamide−Wat51 complex. An alternative model of zinc coordination where the cyanamide molecule was replaced with the standard zinc-bound water molecule has been tested. In this case, the significant residual electron density was always present in the positions corresponding to the C and N2 cyanamide atomic positions and could not be interpreted as additional hydrogen-bonded water molecules.

Figure 1 reports an unbiased omit map calculated with F_c and phases from a final model of the enzyme subjected to two cycles of least-squares refinement after the removal of the cyanamide molecule and Wat51. The structure of the metal site consists of a zinc ion that, besides the three histidine residues, binds one cyanamide molecule at 2.09 Å. The Wat51 molecule approaches zinc at 2.91 Å and can be considered as a zinc outher-sphere fifth ligand resulting in a 4+1 type coordination for the metal ion. Table 2 reports the distances and angles in the zinc coordination polyhedron. The geometry around zinc in the ternary complex cannot be described in terms of the standard square pyramidal or trigonal bipyramidal geometry that is found in five-coordinate complexes. It may be better defined as resulting from the addition of a fifth ligand to the standard zinc coordination tetrahedron of native hCAII. Inspection of the distances in the active site shows that Wat51 is closer to cyanamide (~2.5 Å) than to zinc (2.91 Å). The interaction of cyanamide with hCAII is completed by two strong hydrogen bonds involving Thr199 and Thr200 side chain OH groups and a further H-bond to a water molecule located in the cavity. Table 3 reports the relevant hydrogen bonds in the active site.

Figure 2 shows the zinc coordination and the H-bond pattern linking cyanamide with the Thr199 and Thr200 residues superimposed on the structure of the native hCAII. The free end of the linear cyanamide molecule points toward the opening of the cavity, while Wat51 is located in the hydrophobic pocket of the active site cavity which is defined by residues Val121, Phe131, Leu141,Val143, Leu198, Val207, and Trp209. Wat51 lies ~1.8 Å from the deep water position in the native enzyme and is located about 2.5 Å from the carbon atom of the Zn-bound cyanamide, and the second closest water, about 5.3 Å from the cyanamide carbon, is the cyanamide H-bonded water lying in the opposite direction toward the cavity opening. It is noteworthy that the so-called "deep water" (Wat338 in the 2CBA numbering scheme), always observed buried in the hydrophobic pocket of the native enzyme, is absent in the structure presented here. Upon binding, the cyanamide molecule displaces seven water molecules present in the native structure, whereas all the remaining waters in the cavity are remarkably conserved at the same positions.

Figure 3 reports the superposition of the structure presented here with the hCAII−nitrate complex. The nitrate anion is bound to zinc in a five-coordinate complex where the zinc maintains the native water or hydroxide Wat263 ligand and the nitrate approaches zinc from the hydrophobic pocket with one of its oxygen atoms while a second oxygen is hydrogen bonded to Wat263. The superposition of the hCAII−nitrate complex (*21*) shown in Figure 3 clearly shows that the Wat51 molecule in the structure presented here matches the position occupied by the nitrate oxygen atom weakly bound to zinc in the hCAII−nitrate complex. The same occurs in the thiocyanate−hCAII complex (*22*) where the zinc-bound

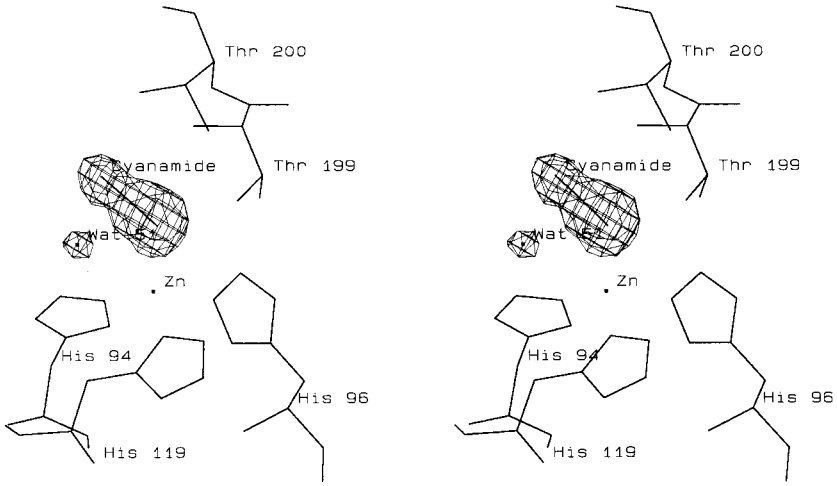

FIGURE 1: Stereoview of the omit map computed with $F_o - F_c$ coefficients and phases calculated after the refinement of the final model from which the Wat51 and cyanamide molecules have been omitted. The map clearly shows the five-coordinate Zn−cyanamide−water adduct.

Table 2: Bond Distances and Angles of the Zn Coordination Polyhedron

		angle (deg)			
	distance from Zn (Å)	X−Zn−His94	X−Zn−His96	X−Zn−His119	X−Zn−N2
His94 Nϵ2	2.00		100.7	122.2	113.8
His96 Nϵ2	2.15			103.7	103.4
His119 Nδ1	2.01				110.2
N2 (cyanamide)	2.09				
Wat51 O	2.91				

Table 3: Selected Distances, with Hydrogen Bond Distances[a] Underlined

N1 cyanamide−Thr200 Oγ	2.84 Å	N2 cyanamide−Thr199 Oγ	2.45 Å
N1 cyanamide−Wat51	2.95 Å	N2 cyanamide−Wat51	2.38 Å
N1 cyanamide−Wat235	2.49 Å	Glu106 Oϵ−Thr199 Oγ	2.54 Å

[a] Hydrogen bonds are assigned on the basis of both distance and geometry criteria.

nitrogen atom of the NCS^- anion approaches the metal ion from the same direction of Wat51.

It is also interesting to compare the cyanamide binding mode with that of the azide anion as observed in several X-ray structures (*23*−*25*). It is evident how the different protonation state of the molecule dictates its orientation within the active site cavity. All the azide molecules point toward the hydrophobic pocket of the cavity because of the hydrogen bond received from the peptide nitrogen of Thr199. On the other hand, cyanamide, because of its protonated nitrogen, is engaged in hydrogen bonds with the Oγ atoms of Thr199 and Thr200 side chains and consequently points in the opposite direction toward the cavity opening. The role of the Thr199 Oγ atom in discriminating and orienting the nonprotein ligand to zinc has been recognized (*26*). Indeed, Thr199 Oγ is engaged in a strong hydrogen bond with the deprotonated side chain of Glu106 that allows it only to act as a hydrogen bond acceptor in a second hydrogen bond involving any protonated ligand bound to zinc.

Figure 4 shows the active site structures of the hCAII−urea complex (*6*) superimposed by least-squares fitting with the structure presented here. The urea and cyanamide molecules lie in the same position with respect to the cavity. Urea binds zinc through a nitrogen atom, which furthermore is engaged in hydrogen bonds with the side chain of Thr199 and with the so-called deep water molecule. The second nitrogen atom of urea is engaged in hydrogen bonds with the side chain of Thr200, and with two water molecules, whereas the urea oxygen atom is hydrogen-bound to Thr200, and two additional waters. It must be remembered that in the urea−hCAII complex the deep water is clearly visible in the usual position within the hydrophobic pocket.

The difference Fourier maps further revealed the presence of a strong electron density peak (20σ) close to the imidazole ring of His64. This density has a spherical shape and lies in a position where an alternative conformation of the His64 side chain is often found (*14*, *27*), and we have interpreted this density as a mercury atom (Hg263) bound 2.5 Å from the Nδ1 atom of the His64 imidazole ring adopting the "inward" conformation, but with the ring plane rotated 180° from its position in the 2CBA structure so that Nδ1 points toward the cavity opening. The putative Hg(II) ion displays an almost regular tetrahedral coordination completed by binding to the carbonyl oxygen of Asn62 and two water molecules. The Hg263 bond distances range between 2.5 and 2.9 Å. The Hg(II) ion has been previously observed bound to His64 at the same position in the hCAII−AMS complex (*22*).

DISCUSSION

The crystallographic analysis presented here points to the presence of two different structures in the hCAII crystals treated with cyanamide under our experimental conditions. The higher-occupancy form shows that cyanamide is able to replace the zinc-bound water or hydroxide molecule of the native enzyme, maintaining the tetrahedral geometry around the metal ion. This form, in our opinion, is hardly

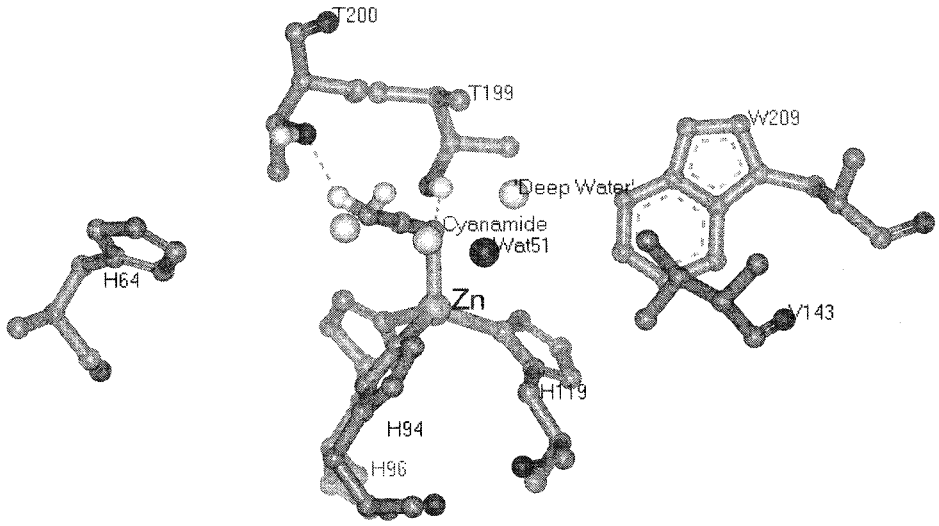

FIGURE 2: Active site of the ternary hCAII−cyanamide−water complex. Three relevant water molecules of the native hCAII structure (2CBA) are shown superimposed as white spheres of arbitrary radius. Wat51 is shown as a gray sphere. The hydrogen bonds linking the cyanamide substrate to the side chains of Thr199 and Thr200 are also shown. The hydrogen atoms relevant to the hydrogen bonding pattern are represented as small white spheres.

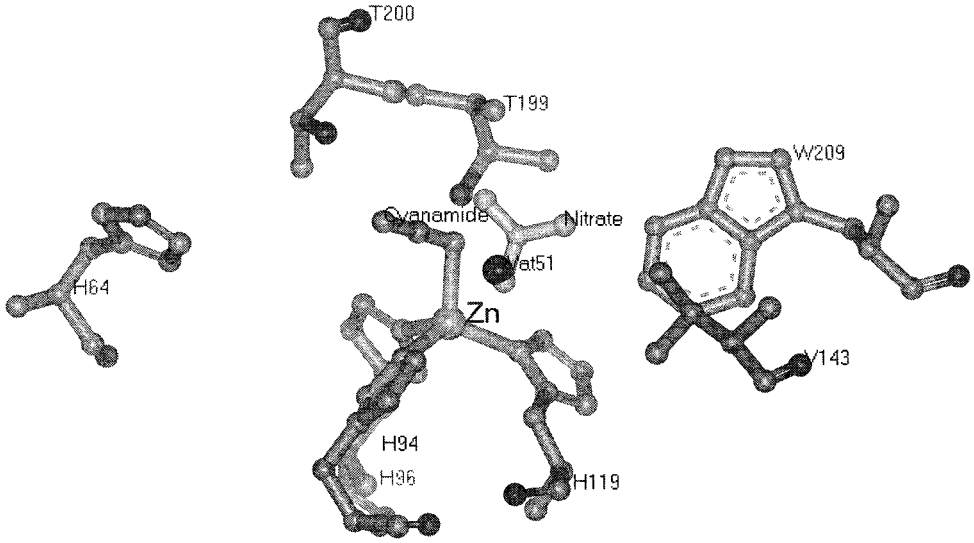

FIGURE 3: Least-squares superposition of the ternary hCAII−cyanamide−water complex with the nitrate anion from the hCAII−nitrate complex [1CAN (*21*)]. It can be seen that the Wat51 position almost exactly matches the position of the zinc-coordinated nitrate oxygen atom. Wat51 is in a proper position to perform a nucleophilic attack on the activated carbon atom of the cyanamide molecule.

consistent with the subsequent evolution of the hydration reaction, as no activated water is present on the metal ion. We therefore consider this adduct as a dead-end product.

The second form of the hCAII−cyanamide complex that could be detected in the solid state refers to a ternary hCAII−cyanamide−water or hydroxide complex (Wat51) that can be interpreted as a frozen intermediate state of the hCAII-catalyzed conversion of cyanamide to urea. Wat51 can be considered to be added to the Zn(II) coordination sphere building up a five-coordinate site. The coincidence of the Wat51 position with that of the zinc-bound oxygen and nitrogen atoms of the five-coordinated adducts with nitrate and thiocyanate, respectively (Figure 3), confirms that this is the site where the fifth ligand may approach the zinc ion, the rest of the coordination sphere of Zn(II) being quite rigidly imposed by the disposition of the three histidine side chains and by the strong hydrogen bonds that hold the fourth nonprotein ligand. Another interesting observation is that in all the five-coordinate hCAII complexes so far crystallogaphically determined (hCAII−thiocyanate, hCAII−nitrate, and hCAII−cyanamide), the deep water has been displaced from its usual binding pocket. It is tempting to speculate that in the structure presented here, Wat51 is the deep water that has moved by about 2.0 Å to approach Zn(II) and cyanamide and that it may actually be the nucleophile converting the zinc-activated cyanamide to urea. In this hypothesis, Figures 3 and 4 can be seen as snapshots along the rection coordinate of the hCAII-catalyzed cyanamide hydration; the water nucleophile approaches zinc from the hydrophobic pocket and attaches the zinc-activated substrate, yielding the urea product.

The possibility of the existence of equilibria between four- and five-coordinate species in CA has been discussed and proved a long time ago (*28*). Formation of a pentacoordinated adduct in the presence of cyanamide was already anticipated on the basis of spectroscopic investigation of Co(II)hCA (*6*). The intensity of the visible electronic spectrum of the enzyme decreases strongly when cyanamide is added to the solution,

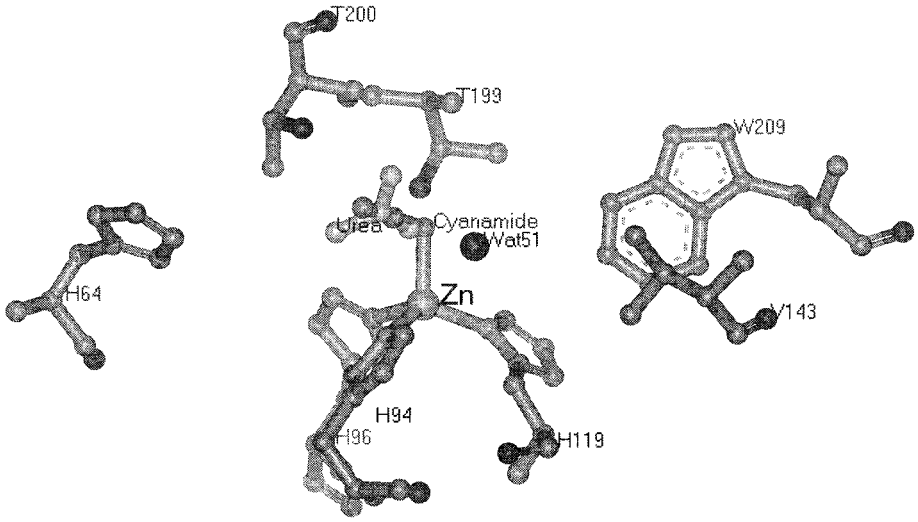

FIGURE 4: Least-squares superposition of the ternary hCAII−cyanamide−water complex with the urea (light gray) from the 1BV3 structure. The product urea occupies the same site of the substrate cyanamide in the zinc coordination polyhedron.

indicating that cyanamide is binding to the metal increasing the coordination number from four to five. The five-coordinate adduct visualized in our structure is likely to represent the productive form which can further evolve toward the formation of urea. Indeed, this form allows a close proximity between the metal-bound activated substrate and the water molecule, which is also bound to the same center. The nucleophilic attack of the water is therefore made more easy, and this five-coordinate complex, therefore, represents a transient species. Once the urea is formed, it remains bound to the metal, inhibiting the enzyme, but still allowing a water molecule to occupy the deep water site.

If the hypothesis described above is true, the cyanamide hydration by hCAII would follow a different mechanism with respect to CO_2 hydration (*5*, *29*). Carbon dioxide, at variance with cyanamide, it is not bound to the metal but is located in the nearby hydrophobic pocket. The proximity to the zinc-bound hydroxide group allows the nucleophilic attack to the CO_2 carbon atom. It has been known for a long time that the CO_2 binding site in this enzyme is rather exclusive, the largest part of inhibitors, including cyanamide itself, being noncompetitive inhibitors. It can be speculated that the very high turnover number observed in the case of CO_2 is, besides other factors, also related to the fact that only weak chemical interactions are necessary for this substrate to be held in proximity to the nucleophilic group, decreasing the energy barrier of the transition state. On the contrary, in the hCAII-catalyzed hydration reaction of cyanamide to urea, Wat51 appears to be the actual nucleophile attacking the metal-activated substrate. Here the role of zinc in the precatalytic step would be mainly that of activating the substrate by polarizing the cyanamide carbon−nitrogen bond, rather than providing the nucleophile. The very slow rate of the cyanamide reaction is then easily explained by considering the difficulty the substrate has in replacing the zinc-bound hydroxide anion and by the fact that Wat51 can be only partially activated by the interaction with the metal.

In conclusion, this is the first X-ray structure of a transient five-coordinate adduct of CA with a molecule which is subsequently hydrated, which provides hints about the possibility that different mechanisms of hydration reactions may operate in human carbonic anhydrase depending on the substrate electronic and stereochemical properties.

ACKNOWLEDGMENT

We thank Dr. Silvia Tilli from the Department of Chemistry of the University of Florence for the help in the enzyme preparation and purification.

REFERENCES

1. Hewett-Emmett, D., and Tashian, R. E. (1996) *Mol. Phylogenet. Evol. 5*, 50−77.
2. Supuran, C. T. (1994) in *Carbonic Anhydrase and Modulation of Physiologic and Pathologic Processes in the Organism* (Puscas, I., Ed.) pp 29−111, Helicon, Timisoara, Romania.
3. Scozzafava, A., Menabuoni, L., Mincione, F., Briganti, F., Mincione, G., and Supuran, C. T. (1999) *J. Med. Chem. 42*, 2641−2650.
4. Christianson, D. W., and Fierke, C. A. (1996) *Acc. Chem. Res. 29*, 331−339.
5. Lindskog, S. (1997) *Pharmacol. Ther. 74*, 1−20.
6. Briganti, F., Mangani, S., Scozzafava, A., Vernaglione, G., and Supuran, C. T. (1999) *J. Biol. Inorg. Chem. 4*, 528−536.
7. Scozzafava, A., Briganti, F., Mincione, G., Menabuoni, L., Mincione, F., and Supuran, C. T. (1999) *J. Med. Chem. 42*, 3690−3700.
8. Supuran, C. T., Scozzafava, A., Menabuoni, L., Mincione, F., Briganti, F., and Mincione, G. (1999) *Eur. J. Pharm. Sci. 8*, 317−328.
9. Petsko, G. A., and Ringe, D. (2000) *Curr. Opin. Chem. Biol. 4*, 89−94.
10. Forsman, C., Behravan, G., Osterman, A., and Jonsson, B. H. (1988) *Acta Chem. Scand. B 42*, 314−318.
11. Behravan, G., Jonasson, P., Jönsson, B. H., and Lindskog, S. (1991) *Eur. J. Biochem. 198*, 589−592.
12. Khalifah, R. G., Strader, D. J., Bryant, S. H., and Gibson, S. M. (1977) *Biochemistry 16*, 2241−2247.
13. Henderson, L. E., Henriksson, D., and Nyman, P. O. (1976) *J. Biol. Chem. 251*, 5457−5463.
14. Håkansson, K., Carlsson, M., Svensson, A., and Liljas, A. (1992) *J. Mol. Biol. 227*, 1192−1204.
15. Collaborative Computational Project, No. 4.1 (1994) *Acta Crystallogr. D50*, 760.
16. Jones, T. A. (1978) *J. Appl. Crystallogr. 11*, 268−272.
17. Jones, T. A., Cowan, S. W., and Kjeldgaard, M. (1991) *Acta Crystallogr. A47*, 110−119.
18. Murshudov, G. N., Vagin, A. A., and Dodson, E. J. (1997) *Acta Crystallogr. D53*, 240−255.

19. Lamzin, V. S., and Wilson, K. S. (1993) *Acta Crystallogr. D49*, 129−147.
20. Laskowski, R. A., MacArthur, M. W., Moss, D. S., and Thornton, J. M. (1993) *J. Appl. Crystallogr. 26*, 283−291.
21. Mangani, S., and Håkansson, K. (1992) *Eur. J. Biochem. 210*, 867−871.
22. Eriksson, A. E., Kylsten, P. M., Jones, T. A., and Liljas, A. (1988) *Proteins*: *Struct., Funct., Genet. 4*, 283−293.
23. Nair, S. K., and Christianson, D. W. (1993) *Eur. J. Biochem. 213*, 507−515.
24. Jönsson, B. M., Håkansson, K., and Liljas, A. (1993) *FEBS Lett. 322*, 186−190.
25. Briganti, F., Mangani, S., Orioli, P., Scozzafava, A., Vernaglione, G., and Supuran, C. T. (1997) *Biochemistry 36*, 10384−10392.
26. Xue, Y., Liljas, A., Jönsson, B.-H., and Lindskog, S. (1993) *Proteins*: *Struct., Funct., Genet. 17*, 93−106.
27. Nair, S. K., and Christianson, D. W. (1991) *J. Am. Chem. Soc 113*, 9455−9458.
28. Bertini, I., Luchinat, C., and Scozzafava, A. (1982) *Struct. Bonding 48*, 45−92.
29. Lindskog, S., and Liljas, A. (1993) *Curr. Opin. Struct. Biol. 3*, 915−920.

BI000937C